

## Article

# Genome-Wide Identification and Expression Analysis of WRKY Genes during Anthocyanin Biosynthesis in the Mango (*Mangifera indica* L.)

Bin Shi <sup>1,2,3,†</sup>, Hongxia Wu <sup>4,†</sup>, Wencan Zhu <sup>1,2,3</sup>, Bin Zheng <sup>4</sup> , Songbiao Wang <sup>4</sup>, Kaibing Zhou <sup>1,2,3</sup>  and Minjie Qian <sup>1,2,3,\*</sup> 

<sup>1</sup> College of Horticulture, Hainan University, Haikou 570228, China; shibin@hainanu.edu.cn (B.S.); 21220951310194@hainanu.edu.cn (W.Z.); zkb@hainanu.edu.cn (K.Z.)

<sup>2</sup> Engineering Research Center of Selecting and Breeding New Tropical Crops Varieties, Ministry of Education, Haikou 570228, China

<sup>3</sup> Key Laboratory of Quality Regulation of Tropical Horticultural Crop in Hainan Province, Haikou 570228, China

<sup>4</sup> Ministry of Agriculture Key Laboratory of Tropical Fruit Biology, South Subtropical Crops Research Institute, Chinese Academy of Tropical Agricultural Sciences, Zhanjiang 524013, China; wuhongxia@catas.cn (H.W.); zhengbin@catas.cn (B.Z.); wangsongbiao@catas.cn (S.W.)

\* Correspondence: minjie.qian@hainanu.edu.cn

† These authors contributed equally to this work.



**Citation:** Shi, B.; Wu, H.; Zhu, W.; Zheng, B.; Wang, S.; Zhou, K.; Qian, M. Genome-Wide Identification and Expression Analysis of WRKY Genes during Anthocyanin Biosynthesis in the Mango (*Mangifera indica* L.).

*Agriculture* **2022**, *12*, 821.

<https://doi.org/10.3390/agriculture12060821>

Academic Editors: Sachin Rustgi and Domenico Pignone

Received: 3 May 2022

Accepted: 6 June 2022

Published: 7 June 2022

**Publisher's Note:** MDPI stays neutral with regard to jurisdictional claims in published maps and institutional affiliations.



**Copyright:** © 2022 by the authors. Licensee MDPI, Basel, Switzerland. This article is an open access article distributed under the terms and conditions of the Creative Commons Attribution (CC BY) license (<https://creativecommons.org/licenses/by/4.0/>).

**Abstract:** The WRKY family is one of the largest transcription factor (TF) families in plants and is involved in the regulation of plant physiological processes, such as anthocyanin accumulation. However, little information is known regarding the WRKY genes in the mango. In this study, a total of 87 mango WRKY genes were identified and named *MiWRKY1* to *MiWRKY87*. Phylogenetic results showed that the 87 *MiWRKYs* could be divided into three groups (I, II, III) and five subgroups of group II (II-a, II-b, II-c, II-d, II-e), with high similarity in exon–intron structures and WRKY domain and motif compositions within the same group and subgroup. One tandem duplication (*MiWRKY76* and *MiWRKY82*) and 97 pairs of segmental duplicates were identified in the mango genome. Syntenic analysis showed that mango *MiWRKY* genes had 52 and 69 orthologous pairs with *Arabidopsis* and citrus, respectively. Promoter cis-acting element analysis revealed that *MiWRKYs* contain a large number of elements associated with light signaling, hormonal response, environmental stress, and plant development. Tissue specific expression profiles showed that the expression of *MiWRKY* genes displayed tissue preference. Quantitative-PCR analysis showed that high expression levels of *MiWRKY1*, *MiWRKY3*, *MiWRKY5*, *MiWRKY81*, and *MiWRKY84* were detected in the skin of red mango cultivar, and the expressions of *MiWRKY1* and *MiWRKY81* were up-regulated during light-induced anthocyanin accumulation in the mango, indicating these genes might regulate anthocyanin biosynthesis in the mango. This study provides comprehensive genetic information on the *MiWRKYs* in mango fruit.

**Keywords:** mango; WRKY; genome-wide; phylogenetic analysis; anthocyanin; gene expression

## 1. Introduction

WRKY is a plant-specific zinc-finger transcription factor (TF). It is named this because it contains a highly conserved seven amino acid sequence, WRKYGQK, at its N-terminus [1]. The WRKY domain is a polypeptide sequence composed of approximately 60 conserved amino acid residues [2]. The DNA-binding domain of WRKY TF generally contains a zinc finger structure, C2H2 or C2HC, at the C-terminal [2]. Although the WRKYGQK sequence in the WRKY domain is highly conserved, variants of the sequence (WRKYGKK, WKKYGQK, WRKYSEK, etc.) have been observed in diverse plants [3–5]. Another main feature of WRKY transcription factor is that the coding sequence corresponding to its WRKY

domain contains an intron, but the regulatory mechanism of the intron is still unclear [6]. The WRKY domain of WRKY TF can specifically interact with the (T)(T)TGAC(C/T) sequence (W-box), and TGAC is the core element of W-box. If any nucleotide in the core sequence is replaced, the ability of WRKY to bind to it will be greatly reduced or completely abolished [1].

The research on WRKYs in the plant kingdom started when the first WRKY gene (*SPF1*) was reported in the sweet potato [7]. The identification of WRKY TFs at the whole genome level has been established in diverse plants, including Arabidopsis [3], rice [8], grape [5], cotton [9], pear [10], pineapple [4], and apple [11]. WRKY proteins have been shown to participate in the regulation of plant growth and developmental processes [12–14]. WRKY TFs are also one of the most characteristic classes of stress response TFs in plants. Numerous studies have shown that the WRKY TFs are widely involved in the regulation of plant responses to biotic (bacterial and fungal diseases and insect feeding) and abiotic (wound, drought, cold, heat, and salinity) stresses [15–17].

Moreover, recent studies showed that WRKY also participates in anthocyanin biosynthesis. Anthocyanin is a water-soluble pigment with strong antioxidation capacity beneficial for human health, which is also responsible for the red, blue, or purple colors in fruits and flowers and is synthesized via the phenylpropanoid and flavonoid biosynthesis pathways [18]. The enzymes involved in anthocyanin biosynthesis include phenylalanine ammonia-lyase (PAL), chalcone synthase (CHS), chalcone isomerase (CHI), flavanone 3-hydroxylase (F3H), flavonoid 3'-hydroxylase (F3'H), dihydroflavonol 4-reductase (DFR), anthocyanidin synthase (ANS), and UDP-glucose: flavonoid 3-O-glucosyltransferase (UGT) [19]. In addition, the expression of structural genes is regulated by transcription factors. The most important transcription factors regulating anthocyanin synthesis are R2R3-MYB, bHLH, and WD40, which form the MYB-bHLH-WD40 (MBW) complex to activate the expression of structural genes [20,21]. Anthocyanin accumulation is regulated by both developmental stages and environmental factors [22], and a large number of TFs are involved in these processes, such as HY5 [23], NAC [24], SPL [25,26], ERF [27,28], BBX [29,30], and MADS box [31]. It has also been shown that WRKY TFs participate in anthocyanin accumulation in different tissues [32–34] or are induced by wounding and light treatment [35–38] via interactions with the MYB, bHLH, or WD40 proteins or by binding to the W-box in the promoter region of anthocyanin biosynthetic genes or regulatory genes to up-regulate their expressions to promote anthocyanin biosynthesis.

The mango (*Mangifera indica* L.) is the fifth largest fruit production in the world, and it has been given the title “King of Tropical Fruits” because of its rich nutrition and unique flavor [39]. Ripe mango fruit exhibits green, yellow, orange, peachy, or dark red skin color, and consumers prefer to choose reddish mangoes. The red coloration of mango peel results from anthocyanin accumulation and cyanidin-3-O-galactoside is the predominant anthocyanin compound in the mango [40]. It is therefore of fundamental and practical significance to improve the red coloration and reveal the regulation mechanism of anthocyanin biosynthesis in the mango. Currently, research about mango anthocyanin biosynthesis mainly focuses on the downstream structural genes and MBW TFs [41–44], while the involvement of upstream TFs, such as WRKY, are still unknown. The genome sequencing of the mango was completed in 2020, providing great opportunities for molecular biology research in the mango [45].

In this study, the whole genome-wide identification of mango WRKY gene family members was completed, and the structural characteristics, subgroup classification, and cis-acting element in the promoter region of *MiWRKYs* were systematically analyzed. Then, the expression patterns of *MiWRKYs* in different tissues (mature leaf, bark, seed, root, flower, peel, and flesh), in different skin-colored cultivars (red, yellow, and green) and during light-induced anthocyanin biosynthesis were analyzed. The results of our study can provide valuable clues for studying the biological function of *MiWRKY* TFs in mango anthocyanin accumulation.

## 2. Materials and Methods

### 2.1. Identification and Annotation of Mango WRKY Genes

The complete genome and proteome sequences and GFF (annotation information) of the mango were downloaded from The National Genome Science Data Center (<https://bigd.big.ac.cn/search?dbId=gwh&q=PRJCA002248>, accessed on 1 January 2022). The AtWRKY protein sequences of *Arabidopsis thaliana* were derived from the TAIR database (<https://www.arabidopsis.org/>, accessed on 1 January 2022). Two different approaches were taken to search for the *Mangifera indica* (Mi) WRKY members. First, the AtWRKY protein sequence was used as a reference to run the Blast in TBtools to align it to all the protein sequences of the mango, and then de-redundancy was performed to obtain the MiWRKY candidates [46]. The online tool NCBI blastp was used to compare to the Swiss-Prot database to remove near-source genes. Finally, NCBI cd-search online sites were used for conserved domain analysis to determine the members of MiWRKY. Meanwhile, hidden Markov model (HMM) of WRKY domain (PF03106) was obtained from the Pfam database (<http://pfam.xfam.org/>, accessed on 1 January 2022), and HMMER 3.0 was used to search for MiWRKY in the mango genome database. The default parameter of cutoff value was set to 0.01. All possible candidate genes were confirmed by the PFAM and SMART programs. The HMMER results were further checked, and then a manual check was performed to ensure that the predicted WRKY domain had a N-terminal conserved heptapeptide sequence (WRKYGQK) and a C-terminal zinc-finger-like motif. The redundant sequences were discarded. Finally, all the MiWRKY genes were identified in the mango genome.

### 2.2. Phylogenetic Tree Construction and Sequence Analysis

All the WRKY domain amino acid sequences of predicted MiWRKY proteins were included in the alignments of multiple MiWRKYs using Jalview [47]. MEGA X was used to build the phylogenetic tree using the conserved domains of MiWRKYs, and the conserved WRKY domains of eight AtWRKY proteins from different groups were selected as references to classify the MiWRKYs [48]. The neighbor-joining (NJ) method was used for building the phylogenetic tree, and the bootstrap was set to 1000 times. The WRKY domains of AtWRKYs and MiWRKYs used for the phylogenetic tree are listed in Supplementary File S1. At the same time, unrooted phylogenetic analysis of the full-length MiWRKY protein sequences was conducted using MEGA X with the maximum likelihood (ML) method. The coding sequences (CDS) of MiWRKY were compared with full-length sequences to identify exon and intron organizations of MiWRKYs using the Gene Structure Display Server (GSDS) for the visualization of gene features. We surveyed up to 10 motifs in the MiWRKY proteins using MEME-suite (<http://meme-suite.org/tools/meme>, accessed on 3 January 2022). Finally, the conserved domains, conserved motifs, and seqlogo plots were drawn using TBtools [46].

### 2.3. Chromosomal Distribution and Syntenic Analysis

The chromosome location and gene duplication analysis of the MiWRKY genes were conducted using TBtools based on the annotation file of the mango genome (GFF) [46]. Syntenic analysis of WRKY genes in the mango, *Arabidopsis thaliana* and *Citrus sinensis* was conducted by the TBtools software, which embeds MCscan X software with the default parameters [46,49]. The genome of *Arabidopsis thaliana* and *Citrus sinensis* were downloaded from the Arabidopsis (<https://www.arabidopsis.org/>, accessed on 3 January 2022) and citrus (<http://citrus.hzau.edu.cn/orange/>, accessed on 3 January 2022) databases, respectively.

### 2.4. Promoter Cis-Acting Element Analysis

The 2000 bp sequence upstream of the start codon 'ATG' at the 5' end of the MiWRKY genes was regarded as a candidate promoter, and related cis-acting elements were analyzed using the PlantCare website (<https://bioinformatics.psb.ugent.be/webtools/plantcare/html/>, accessed on 3 January 2022). All cis-acting elements were classified into four groups:

light-responsive elements, development-related elements, hormone-responsive elements, and environmental-stress-related elements.

### 2.5. Plant Materials and Treatments

Five mango cultivars were used in this study, namely ‘Hongmang NO.6’, ‘Sensation’, ‘Geifei’, ‘Jinhuang’, and ‘Qingmang’. They were harvested from the South Subtropical Crops Research Institute (SSCRI) in Zhanjiang, China.

For the bagging treatment, three mature ‘Sensation’ trees were selected for uniform exposure to sunlight, and all three trees were close in size and number of fruits, with each tree considered as a biological replicate. On each tree, approximately 50 fruits were covered with double yellow and black paper bags (Qingdao Kobayashi Co., Ltd., Qingdao, China) to filter all light at 20 days after full bloom (DAFB). The remaining non-bagged fruits served as controls. Ten mangoes were harvested at three developmental stages (50, 80, and 120 DAFB) per tree, kept in an ice box, and transported to the laboratory quickly. The peels were collected and immediately frozen in liquid nitrogen and stored at  $-80^{\circ}\text{C}$ .

For postharvest UV-B/visible light exposure, three similar trees of ‘Hongmang NO.6’ were chosen. The amount of 90 fruits per tree were bagged, as described above, and green mature fruits were harvested with their bags. A total of 180 uniform, defect-free fruits were randomly divided into two groups and kept in plant growth chambers (Conviron, Adaptis A 1000, Winnipeg, MB, Canada) with the temperature of  $17^{\circ}\text{C}$  and relative humidity of 80%. A total of 90 fruits were kept in dark as the controls, 90 fruits were exposed to UV-B/visible light, and 30 fruits per each group were regarded as one biological replicate. Visible and UV-B light were generated by 12 fluorescent tubes (Guangdong PAK Lighting Technology Co., Ltd., 28W/T5, Guangzhou, China), and one narrowband UV lamp (PHILIPS PL-S 9W/01, 311 nm, Amsterdam, Holland), respectively. The intensity of visible and UV-B light were 4000 Lux and  $4.5 \mu\text{W}\cdot\text{cm}^{-2}$ , respectively. Samples were collected at 0, 6, 24, 72, 144, and 240 h of UV-B/visible light treatment for anthocyanin measurement and RNA extraction.

To compare the anthocyanin accumulation pattern among different cultivars, ‘Geifei’ (red skin), ‘Jinhuang’ (yellow skin), and ‘Qingmang’ (green skin) were used as materials. Three trees per cultivar were selected as three biological replicates. For each tree, eight ripe fruits free from insect damage or mechanical damage were harvested. The fruit peels were sampled and stored at  $-80^{\circ}\text{C}$  for subsequent analysis.

### 2.6. Acquisition and Analysis of RNA-Seq Data

In this study, we used a total of two sets of transcriptomic data. Transcriptomic data of different tissues of the ‘Alphonso’ mango, including mature leaf, bark, seed, root, flower, peel, and flesh, were downloaded from the NCBI database (accession number: PRJNA48715). The peels of the ‘Sensation’ mango from the ‘bagging treatment experiment’ which had been described above were used for RNA-Seq by Metware Biotechnology Co., Ltd. (Wuhan, China). Total RNA was extracted, and mRNA was enriched, fragmented and reverse-transcribed to cDNA. The double-stranded cDNA was purified by AMPure XP beads, repaired at the end, A-tail added, and ligated to the sequencing adapters. After approximately 200 bp of cDNA being screened by AMPure XP beads, cDNA was enriched by PCR amplification to obtain the final cDNA library. RNA sequencing was based on the Illumina sequencing platform, using a two-end sequencing (paired-end) approach. The raw data was filtered to remove the low-quality data and to acquire the clean reads by Fastp software (<https://github.com/OpenGene/fastp>, accessed on 10 January 2022). The clean reads were mapped to the mango reference genome (BIG Genome Sequence Archive database, accession number: PRJCA002248) using TopHat [50]. The reads were assembled to transcripts by Cufflinks and gene expression was calculated as Fragments Per Kilobase of transcript per million fragments mapped (FPKM) = mapped fragments of transcript/[total count of mapped fragments (millions)  $\times$  length of transcript (kb)] [50].

### 2.7. Measurement of Anthocyanin Content of Mango Peel

The total anthocyanin content was measured according to the protocol by Kanzaki et al. [41]. Anthocyanin of 0.1 g fruit peel was extracted using 1 mL methanol (with 0.01% HCl) for 72 h at 4 °C in darkness. The resulting solution was centrifuged for 10 min at 12,000 rpm and 4 °C, and the supernatant was spectrophotometrically measured at 530 nm using a New Century T6 spectrophotometer (New Century, Beijing, China). All measures were done in three biological replicates.

### 2.8. RNA Extraction and Gene Expression Analysis

RNA prep pure plant kit (Tiangen, DP441, Beijing, China) was used for RNA isolation. Genomic DNA was digested by DNaseI, and the concentration of total RNA was determined using a NanoDropLite spectrophotometer (Thermo Scientific, Waltham, Massachusetts, USA). An amount of 1 µg of total RNA was reverse-transcribed to cDNA using the HiScript IIQ RT SuperMix (Vazyme, R223-01, Nanjing, China). The cDNA was diluted 20 times and used as a template for Q-PCR. The Q-PCR reaction solution (total volume 15 µL) consisted of 7.5 µL SYBR premix ExTaqTMII (Takara, Japan), 1 µL of both forward and reverse primers (10 µM) and 5.5 µL of cDNA. A real-time PCR machine (qTOWER3G, Jena, Germany) was used for the Q-PCR reaction, initiated at 95 °C for 30 s and then followed by 40 cycles of 95 °C for 5 s and 60 °C for 30 s. All the Q-PCR primers for the genes are shown in Supplementary File S2. Gene expression was analyzed using the  $2^{-\Delta\Delta C_t}$  method, with the normalization by the mango *actin* gene. All samples were set up in three biological replicates.

### 2.9. Statistical Analysis

The experimental data was statistically analyzed by a one-way analysis of variance (ANOVA), and Tukey's multiple range test was used for mean value separation by SPSS 19.0 (SPSS, Chicago, IL, USA). *p*-value of <0.05 was considered statistically significant.

## 3. Results

### 3.1. Identification, Multiple Sequence Alignment and Phylogenetic Analysis of MiWRKY Proteins

In total, 87 MiWRKYs were identified, named MiWRKY1 to MiWRKY87 in the order of increasing E-value by the HMMER search. The shortest protein contained 136 amino acids (MiWRKY13), while the longest protein had 749 amino acids (MiWRKY87) (Supplementary File S3). The WRKY domains of 87 MiWRKY and 9 AtWRKY proteins were used to construct a phylogenetic tree, and the MiWRKYs were classified into three major groups (I, II, III) and five subgroups of group II (II-a, II-b, II-c, II-d, II-e) (Figure 1). Among the 87 MiWRKY proteins, 17 MiWRKYs belonged to Group I with two WRKY domains and C2-H2 zinc finger motifs, and two WRKY domains were located at the N-terminal (I-NT) and C-terminal (I-CT), respectively (Figure 2a,b). A total of 59 MiWRKYs belonged to Group II with a single WRKY domain and C2-H2 zinc finger motif and were further divided into five subgroups due to the presence of additional structural motifs that were conserved among subsets, with 5 MiWRKYs belonging to II-a, 13 to II-b, 22 to II-c, 8 to II-d, and 11 to II-e (Figure 2c–g). Group III contained 11 MiWRKYs with a single WRKY domain and C2-HC zinc finger motif (Figure 2h).

### 3.2. Gene Structure and Conserved Motif Analysis of MiWRKY Proteins

A phylogenetic tree based on the full-length sequence of MiWRKY proteins showed a similar result with the one constructed by the WRKY domain, i.e., all the MiWRKYs were clustered into three groups and five subgroups of group II (Figure 3a). Conserved motif analysis found that all the MiWRKYs contained motif 1, representing for the WRKY domain, and Group I contained motif 3 for the additional WRKY domain (Figure 3b). Although different MiWRKY proteins contained different motifs, the number, type, and order of motifs showed high similarity with the evolutionarily close MiWRKY proteins (Supplementary File S4). For instance, Group II-c mainly contained motifs 1, 2, and 4, and

the order is fixed, and motif 6 was only present in Group II-a and II-b. Figure 3c showed that there were seven different domain combinations of 87 *MiWRKYs*: WRKY domain + WRKY domain, WRKY domain + plant-zn-clust domain (PF10533), WRKY domain + FlaC-arch domain (PF05377), WRKY domain + PspC domain (PF04024), WRKY domain + bZIP domain (PF00170), WRKY domain + ZapB domain (PF06005), and WRKY domain + Leu\_zip domain (PF15294). The number and types of exons and introns of all the identified *MiWRKY* genes were tested to gain a deeper understanding of the evolution of the mango *WRKY* family. As shown in Figure 3c, 87 *MiWRKY* genes contained two to seven exons (8 with two exons, 40 with three exons, 16 with four exons, 11 with five exons, 11 with six exons, 1 with seven exons). Nonetheless, the number of exons in the same subfamily was relatively stable. For example, the number of exons in Group II-e *MiWRKYs* were three and in Group II-d *MiWRKYs* was three or four. Further analysis indicated that all *MiWRKY* genes contained an intron separating the C-terminal WRKY domain, while there was no intron in the N-terminal WRKY domain in Group-I.

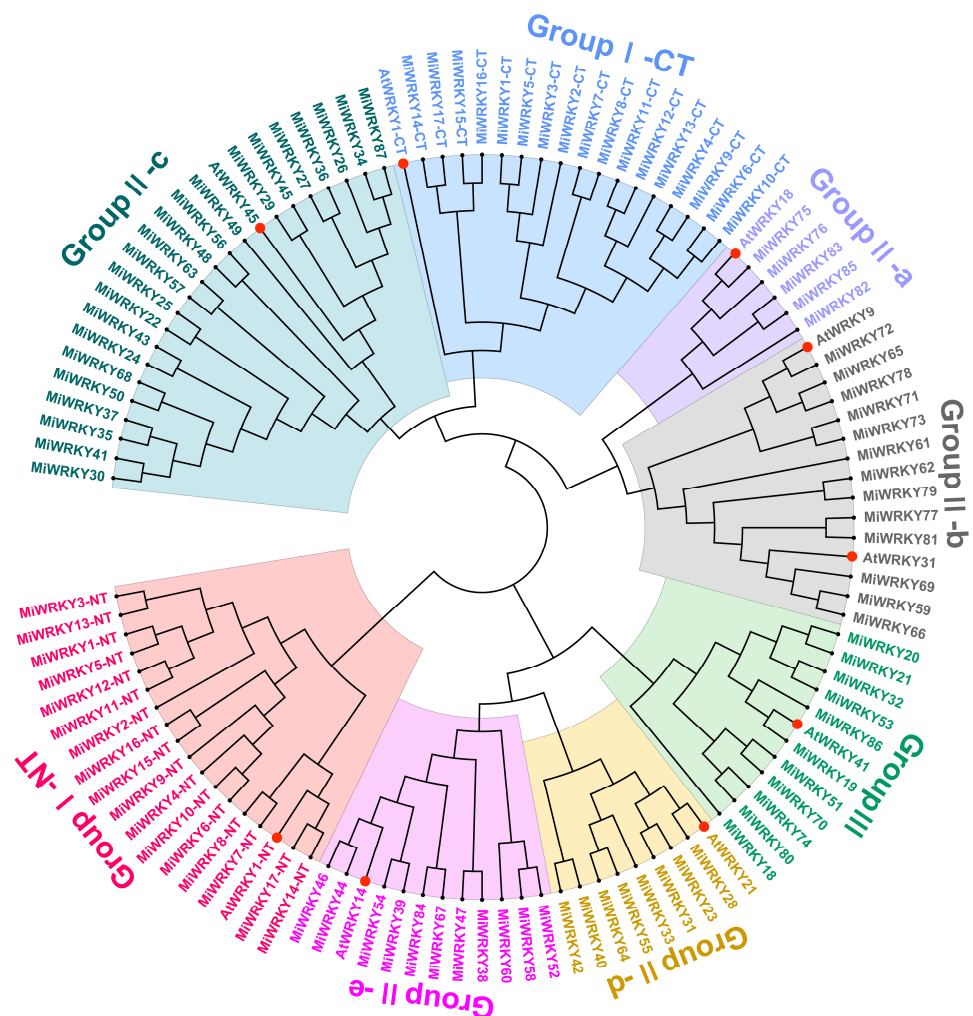


**Figure 1.** Phylogenetic tree of identified *MiWRKY* proteins. Select *AtWRKY* proteins served as representatives for the different groups. Group I to Group III *WRKY* proteins are shown in different colors. The mango and Arabidopsis *WRKY* domains are represented by black solid circles and red circles, respectively. *WRKYs* named with the suffix -NT or -CT represent either the N-terminal *WRKY* domain or the C-terminal *WRKY* domain of *MiWRKY* proteins with two *WRKY* domains.

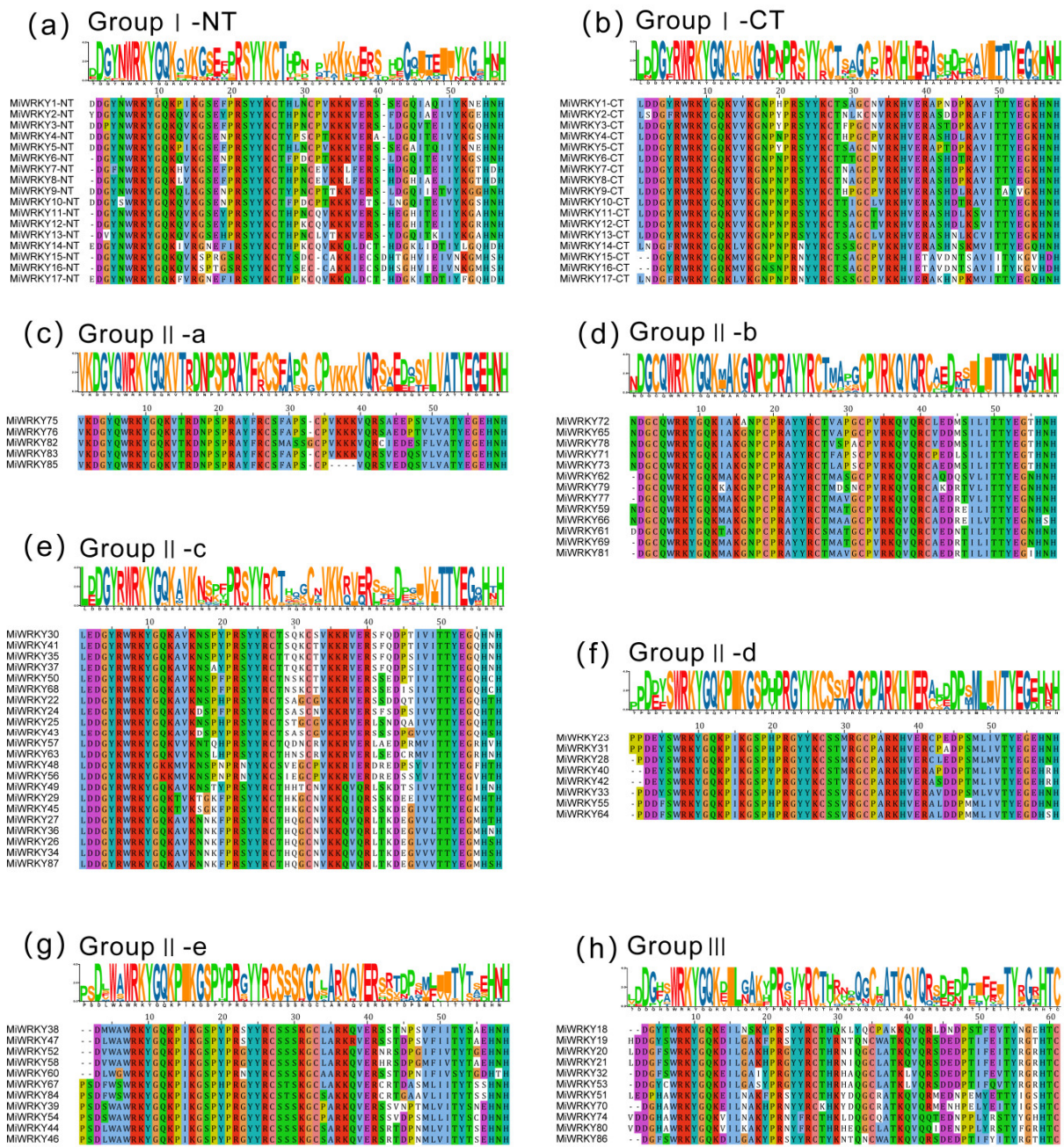


**Figure 2.** Structural domain seqlogo pattern map and multiple sequence alignment results of 87 *MiWRKY* proteins. ‘NT’ and ‘CT’ represented the N- and C-terminal WRKY domains, respectively.

### 3.3. Chromosomal Distribution and Syntenic Analysis of *MiWRKY* Genes

Based on the annotation file of the mango genome (GFF), 86 out of 87 *MiWRKY* genes were mapped to 20 chromosomes (Figure 4a). Only *MiWRKY16* was mapped to Scaffold000224 (Supplementary File S3), which might be caused by the imperfect assembly of the mango genome. Of these, the number of *MiWRKYs* on the chromosomes from lowest to highest was as follows: chromosome 3, 6, and 15 (1 gene); chromosome 14 (2 genes); chromosome 1, 2, 7, 12, 13, and 17 (3 genes); chromosome 8 and 20 (4 genes); chromosome 5, 9, 10, and 18 (5 genes); chromosome 4 (6 genes); chromosome 19 (7 genes); chromosome 11 and 16 (11 genes). *MiWRKYs* of the Group I existed on all the chromosomes except for 3, 6, 7, 8, 12, 13, 15, and 17. *MiWRKYs* of the Group II were distributed on all the chromosomes, and *MiWRKYs* of the Group III were located on chromosomes of 4, 8, 10, 11, 13, 16, 17, 19, and 20 (Figure 4a; Supplementary File S3). According to the descrip-

tion of Holub, chromosomal regions containing more than one gene within 200 KB were defined as tandem duplication event [51]. Genomic duplication event analysis showed that there was one tandem duplication event that happened on Chr05 (*MiWRKY76* and *MiWRKY82*) (Figure 4a; Supplementary File S5). In addition, there were 97 pairs of segmental duplicates involving 76 *MiWRKY* genes identified in the mango genome (Figure 4a; Supplementary File S5). The syntenic relationships of *MiWRKY* genes among the mango (*Mangifera indica*), Arabidopsis (*Arabidopsis thaliana*), and citrus (*Citrus sinensis*) showed that *MiWRKY* genes had 52 orthologous pairs with Arabidopsis, and 69 orthologous pairs with citrus (Figure 4b; Supplementary File S6).

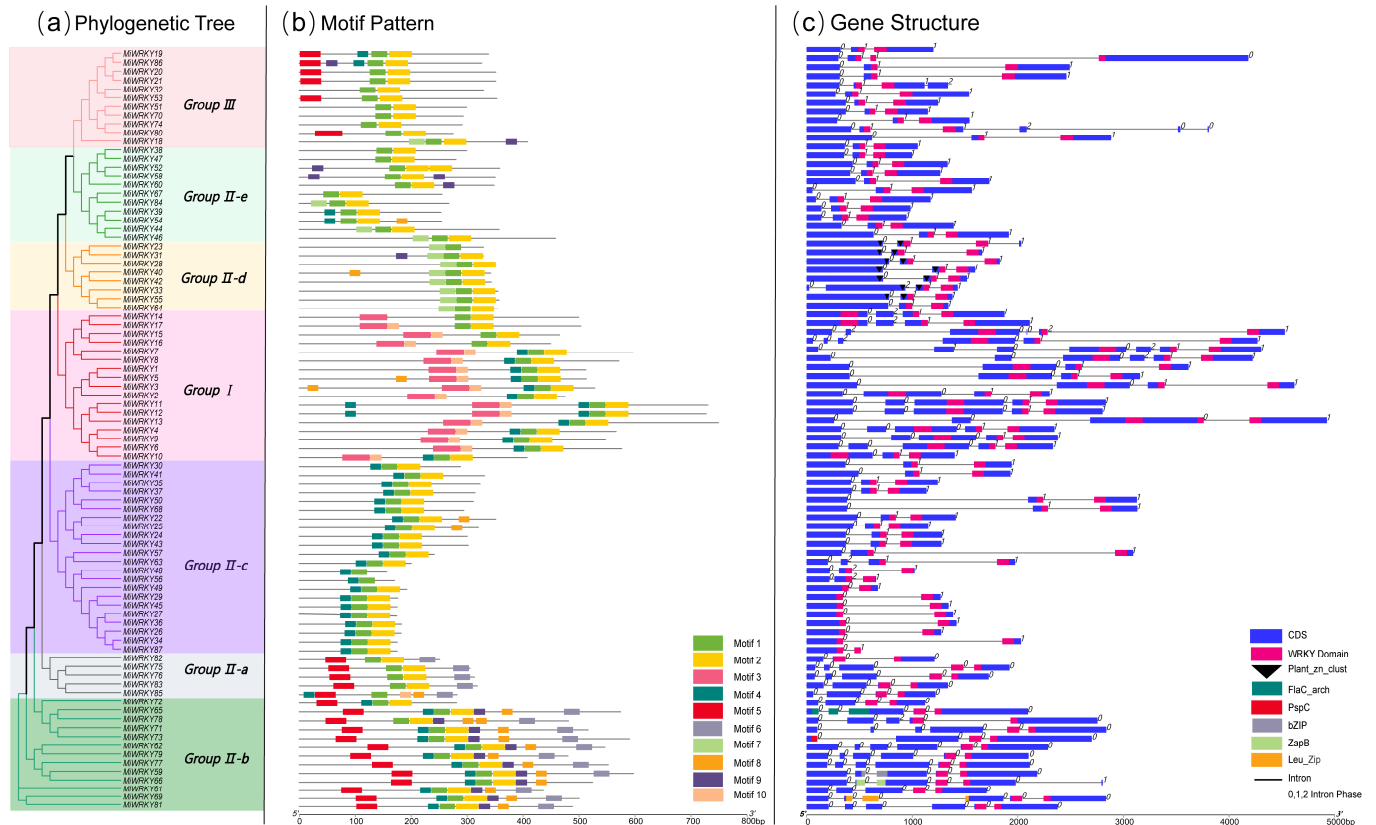


**Figure 3.** Phylogenetic relationships, motif pattern, and gene structure in *WRKY* genes from the mango. (a) Using MEGA-X software, a phylogenetic tree was built according to the full-length sequences of mango *WRKY* proteins. Different colors were used to show the different clusters. (b) Mango *WRKY* protein motif composition. Motifs numbered from 1 to 10 were exhibited with differently colored boxes. Sequence information for each subject is supplied in Supplementary File S4. The scales were used for protein length estimation. (c) Gene structure of mango *WRKY*s. Blue boxes indicated coding sequences (CDS); black lines indicated introns. The *WRKY* domains are shown by red boxes. The numbers show the phases of the corresponding introns.

### 3.4. Cis-Acting Element Analysis of *MiWRKY* Genes

The 2000 bp upstream region of each *MiWRKY*'s translation initiation site was regarded as the promoter and submitted to PlantCARE to search for the cis-acting element. Except for core promoter elements, such as TATA-box, CAAT-box, and some unknown functional elements, all the 45 cis-acting elements were classified into four categories: light-responsive elements (ACE, G-box, AE-box, etc.), hormone-responsive elements (ABRE, AuxRR-core, TGA-box, etc.), environmental-stress-related elements (ARE, MBS, GC-motif, etc.), and development-related elements (CAT-box, RY-element, NON-box, etc.), and the details of all the elements are listed in the Supplementary File S7. The distribution pattern of the cis-elements of *MiWRKY* genes with close evolutionary relationships did not show strong

correlations (Figure 5a). Among all the elements, 1169 light-responsive elements were identified, which was the highest percentage (52.2%), followed by hormone-responsive elements (644, 28.8%), environmental-stress-related elements (333, 14.9%), and development-related elements (94, 4.2%) (Figure 5b).

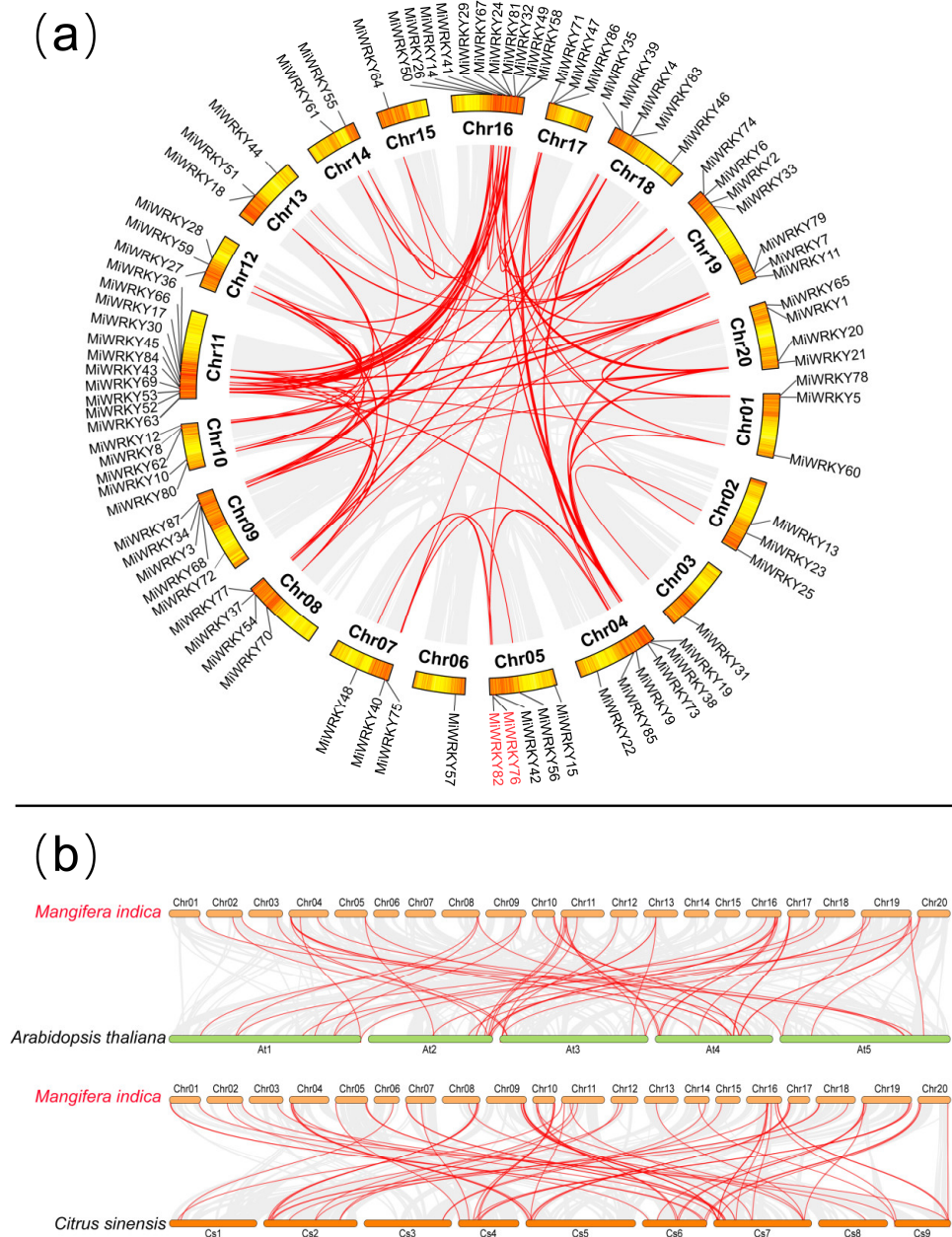


**Figure 4.** The syntenic relationship of *WRKY* genes. (a) The interchromosomal relationship of the *MiWRKY* genes in the mango. Red lines indicate segmental duplicates of *MiWRKY* genes. *MiWRKY76* and *MiWRKY82* marked in red font are defined as tandem duplication events. (b) Collinearity analysis of *WRKY* genes among *Mangifera indica*, *Arabidopsis thaliana*, and *Citrus sinensis*. Red lines highlighted syntenic *WRKY* gene pairs, gray lines indicate collinear blocks within the three species.

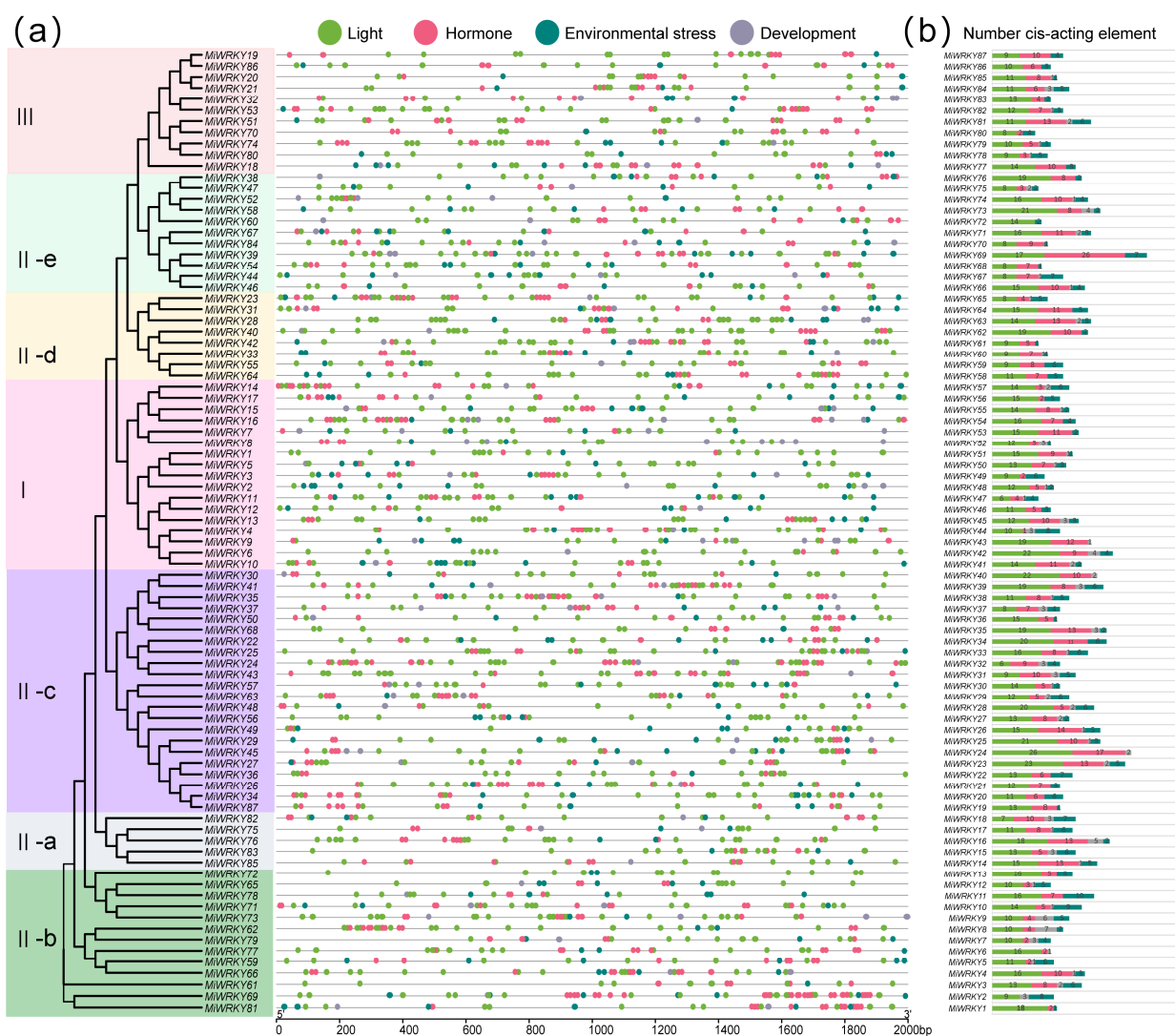


**Figure 5.** Analysis of cis-acting elements in the promoter region of the *MiWRKY* family. (a) The distribution of cis-regulatory elements in the 2000 bp upstream sequences of *MiWRKY* genes promoter region. (b) The numbers of cis-regulatory elements for each *MiWRKY* gene.

### 3.5. Tissue Specific Expression Profiling of *MiWRKY* Genes

The tissue-specific expression pattern of 87 *MiWRKY* genes was analyzed from the transcriptome data of the ‘Alphonso’ mango, including mature leaf, bark, seed, root, flower, peel, and flesh (Figure 6). All the genes were clustered into three groups due to the expression pattern, Group A: 27 genes were highly expressed in most tissues; Group B: 24 genes were highly expressed in specific tissues; Group C: 36 genes were not well-expressed in most tissues. Interestingly, *MiWRKY* genes highly expressed in peels included all the 24 genes in Group A and most genes in Group B except for *MiWRKY87*, *MiWRKY39*, *MiWRKY77*, and *MiWRKY23*. The FPKM of all 87 *MiWRKY* genes in the mango organs/tissues transcriptome data can be found in Supplementary File S8.

### 3.6. Expression Patterns of *MiWRKY* Genes during Anthocyanin Accumulation

Since anthocyanin accumulation of mango is strongly dependent on light, the ‘Sensation’ mango was bag-treated, and RNA sequencing was performed to screen *MiWRKYs* involved in anthocyanin biosynthesis. Compared with bagged fruit peel in which almost no anthocyanin concentration could be detected, fruit grown under natural light showed a high concentration of anthocyanin with the anthocyanin-specific absorbance value at

530 nm, reaching approximately 0.13/g FW (Figure 7a). Based on the transcriptome data, six *MiWRKYs*, including *MiWRKY1*, *MiWRKY2*, *MiWRKY3*, *MiWRKY5*, *MiWRKY81*, and *MiWRKY84*, were selected as candidate light-responsive genes since their expressions were induced by sunlight (Figure 7b). The expressions of these six genes were further confirmed by Q-PCR. The results showed that the transcriptions of six *MiWRKYs* were not correlated to anthocyanin biosynthesis at 50 DAFB. Except for *MiWRKY84*, the transcription levels of the other five *MiWRKYs* were significantly inhibited by the bagging treatment at 120 DAFB (Figure 7b, Supplementary File S9).

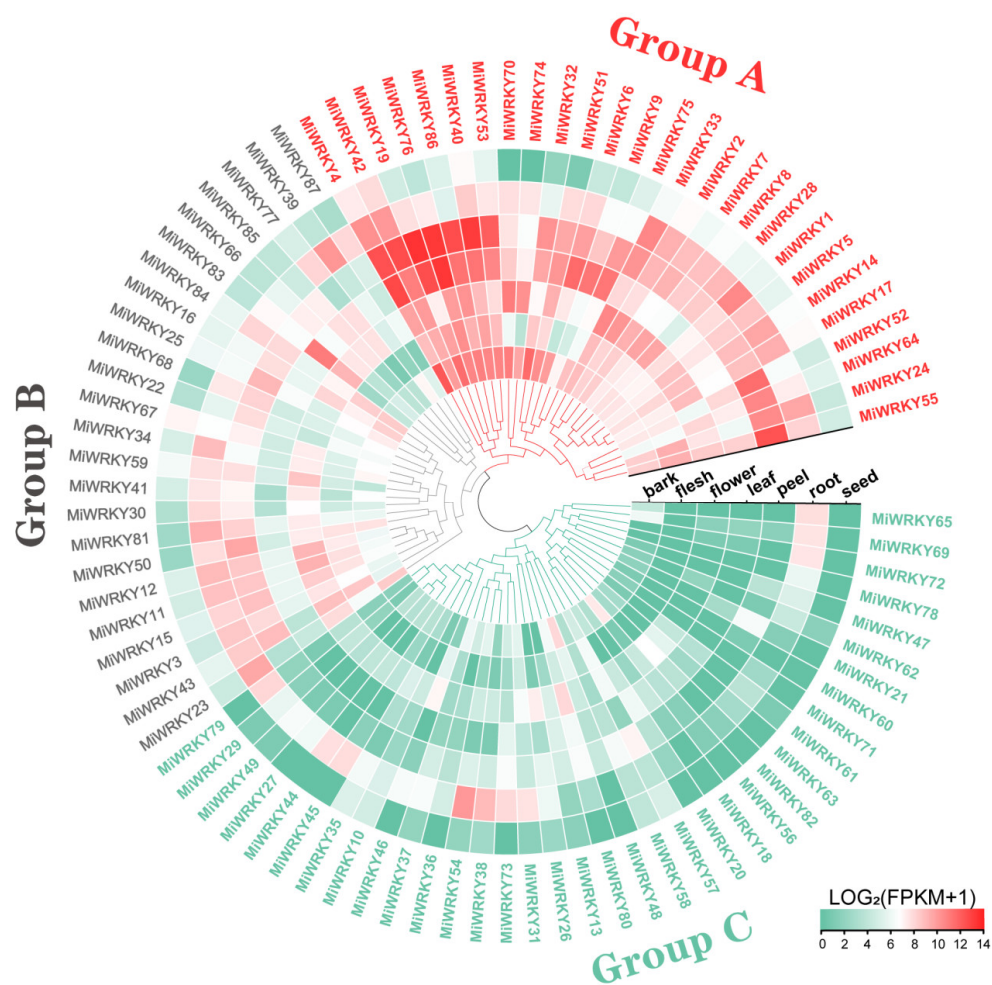


**Figure 6.** Hierarchical clustering of mango WRKY expression profiles in different tissues. The 87 *MiWRKY* genes are divided into Groups A-C. The color bar represents the expression value.

Anthocyanin concentrations and expression patterns of *MiWRKY1*, *MiWRKY2*, *MiWRKY3*, *MiWRKY5*, *MiWRKY81*, and *MiWRKY84* were analyzed by postharvest UV-B/visible light treatment. No anthocyanin content was detected in fruit peel under darkness during the whole period, while the accumulation of anthocyanin in UV-B/visible-light-treated fruit was started at six days of irradiation and peaked at ten days (Figure 8a). Among the six *MiWRKYs*, only *MiWRKY1* and *MiWRKY81* responded to UV-B/visible light treatment. The expressions of these two genes were induced at one day of treatment and remained at high levels afterwards (Figure 8b).

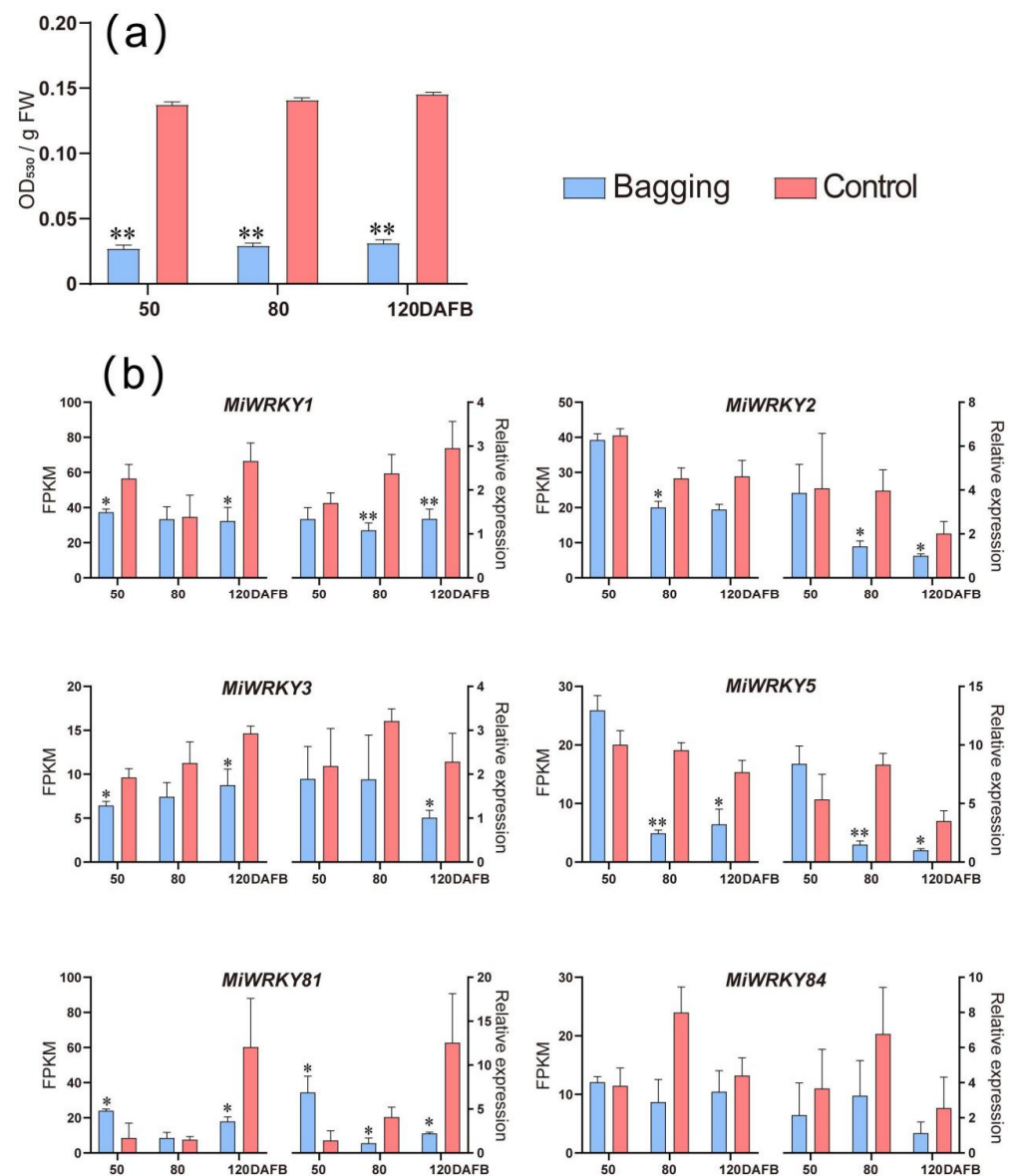


**Figure 7.** (a) The contents of anthocyanin in bag-treated and control ‘Sensation’ mango peel. (b) Q-PCR validation of candidate expressed genes in ‘Sensation’ mango peel detected by RNA-Seq. The RNA-Seq data (left) are shown with the Q-PCR data (right). The data represents the mean  $\pm$  standard deviation with  $n = 3$ . \* represents significant difference ( $p$ -value  $< 0.05$ ); \*\* represents highly significant difference ( $p$ -value  $< 0.01$ ), as determined by Student’s  $t$ -test.

The expression levels of six *MiWRKYs* were also detected in three different colored mango cultivars, including ‘Guifei’ (red), ‘Jinhuang’ (yellow), and ‘Qingmang’ (green) (Figure 9a). The expression of *MiWRKY2* showed no difference among the three cultivars. *MiWRKY2*, *MiWRKY3*, *MiWRKY5*, *MiWRKY81*, and *MiWRKY84* were highly expressed in ‘Guifei’ but were not well expressed in the non-anthocyanin accumulated cultivars, ‘Jinhuang’ and ‘Qingmang’ (Figure 9b).

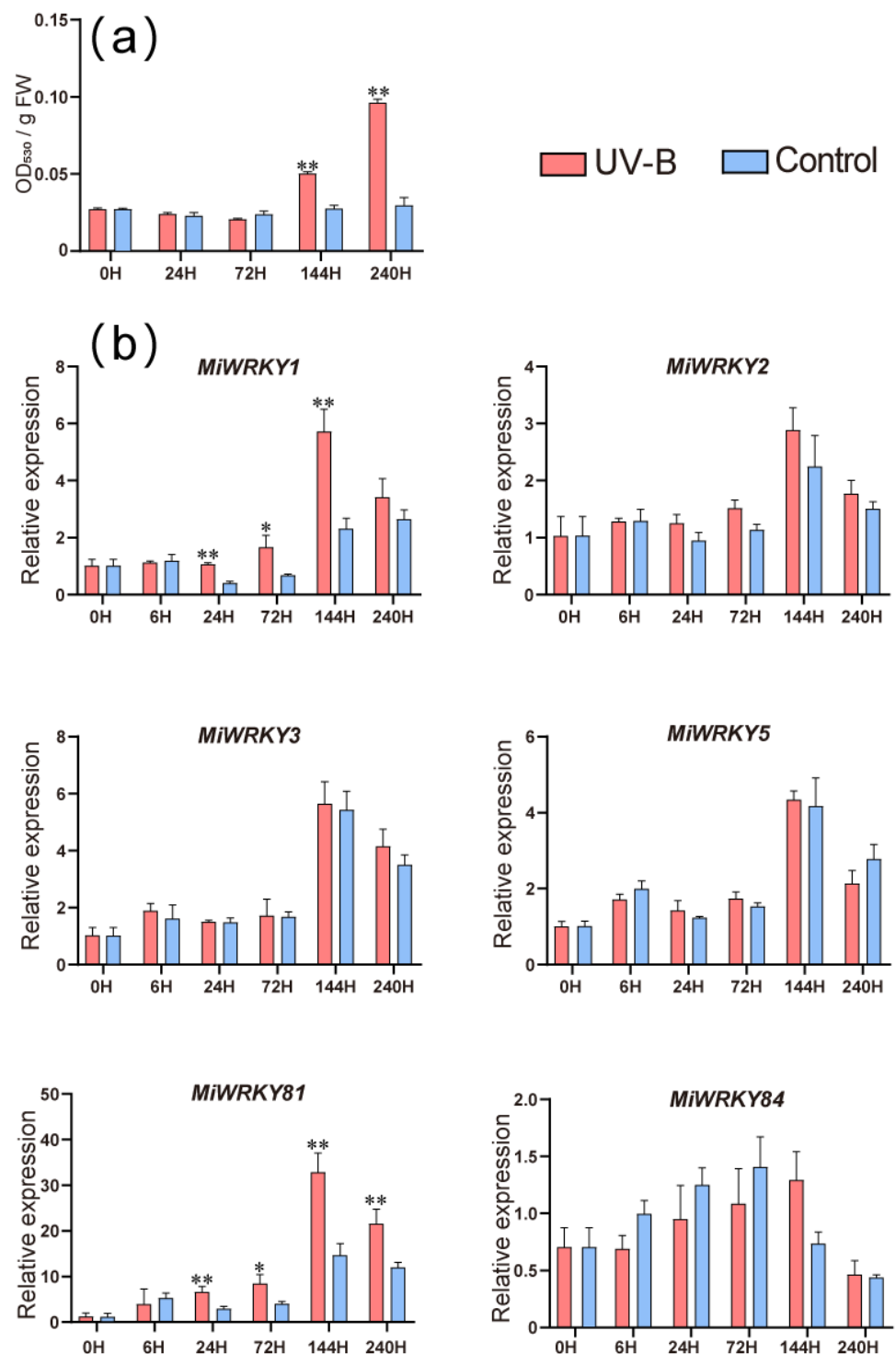


**Figure 8.** (a) The contents of anthocyanin in UV-B/visible light-treated and control (darkness) ‘Hongmang NO.6’ mango peel. (b) Analysis of WRKY genes expression in UV-B/visible-light-treated and control (darkness) ‘Hongmang No. 6’ mango peel. The data represent the mean  $\pm$  standard deviation with  $n = 3$ . \* represents significant difference ( $p$ -value  $< 0.05$ ); \*\* represents highly significant difference ( $p$ -value  $< 0.01$ ), as analyzed by Student’s  $t$ -test.

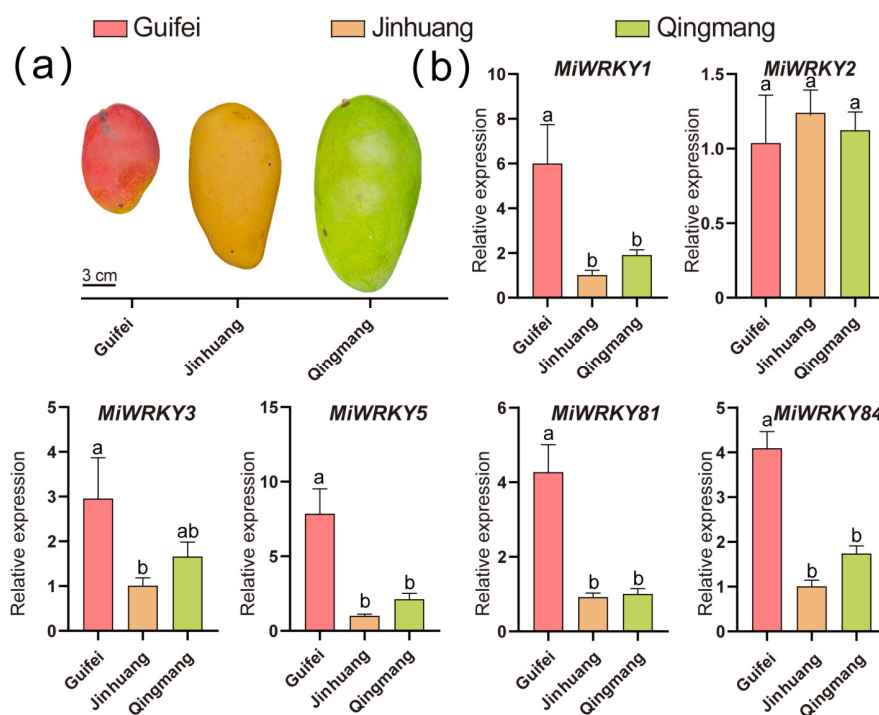


**Figure 9.** (a) Phenotypes of three mango cultivars, including ‘Guifei’ (red skin), ‘Jinhuang’ (yellow skin), and ‘Qingmang’ (green skin). (b) Expression levels of *MiWRKY* genes in ‘Guifei’, ‘Jinhuang’, and ‘Qingmang’ fruit skin. The data represents the mean  $\pm$  standard deviation with  $n = 3$ . Different letters above bars denote significant difference at  $p < 0.05$ .

#### 4. Discussion

WRKY is one of the largest families of transcriptional regulators in plants. With the increasing number of genome-sequenced plant species, genome-wide analysis of the WRKY gene family has been established in various plant species [3,5,8–11,52–54]. In the current study, 87 WRKYs were identified in the mango, named MiWRKY1 to MiWRKY87 on the basis of the order of HMMER retrieval (Figure 1). The number of WRKYs in the mango is comparable to that in rice but smaller than that in Arabidopsis since 72, 100, and 87 WRKYs were identified in Arabidopsis (genome size 125 Mb), rice (480 Mb), and mango (393 Mb), with 0.58, 0.21, and 0.22 WRKY per Mb genome size, respectively [3,45]. The WRKY distribution in different groups also varies among these three species. For instance, rice showed an average distribution with 34%, 30%, and 36% belonging to Group I, Group II, and Group III, respectively, while Arabidopsis and mango showed a lower percentage of Group III WRKYs with 19.4% and 12.6%, respectively (Figure 1) [3]. In addition, Arabidopsis showed a high percentage of Group I WRKYs (44.4%) and Group II WRKYs are the most abundant in the mango (67.8%) (Figure 1) [3]. Group IV WRKYs were found in rice, which contain the WRKY domain but lack a complete zinc-finger motif, probably due to pseudogenes or sequencing and assembly errors [8,55], while no Group IV WRKYs were identified in the mango.

The WRKY domain containing a core WRKYGQK motif is essential for the WRKY protein to bind to the W-box in the promoter region of target genes. In the present study, Group II-C MiWRKY48 and MiWRKY56 showed sequence variation in WRKYGQK motif, where WRKYGQK was replaced by WRKYGKK (Figure 2e), which also occurred in pineapple Group II-C WRKYs (AcWRKY43, AcWRKY28, and AcWRKY23) [4]. Previous studies showed that the WRKYGQK motif variation might affect the interaction between WRKY and its target genes [56–58]; thus, it will be interesting to further analyze the functions and binding specificities of MiWRKY48 and MiWRKY56.

Domain gain and loss is one of the driving forces for WRKY gene family expansion. The two non-photosynthetic organisms of ancient eukaryotes, unicellular protist, *Giardia lamblia*, and slime mold, *Dictyostelium discoideum*, each contain a single WRKY protein with two WRKY domains belonging to Group I, indicating the early evolution and ancestral form of Group I WRKY [3]. WRKY domain loss is common in monocotyledonous plants, including rice and maize, where Group I proteins contain only one WRKY domain, either the C-terminal or the N-terminal domain [3,8,50]. In dicotyledons, such as Arabidopsis, all the WRKY proteins of Group I except AtWRKY10 have two WRKY domains [3], and in the mango, all the identified Group I WRKY proteins contain two WRKY domains (Figure 2a,b), indicating the divergence of the Group I WRKY protein evolution between dicotyledons and monocotyledons. Studies have shown that the DNA-binding function of WRKY transcription factor was mainly mediated by the C-terminal WRKY domain, while the N-terminal WRKY domain might contribute to the binding process or provide an interface for protein–protein interactions, such as some zinc-finger-like domains [59]. In this study, all the WRKY domains of Group II and III showed a closer relationship with the C-terminal WRKY domain of Group I on the phylogenetic tree (Figure 1), indicating these domains share the common function of DNA binding, and the N-terminal WRKY domain evolved to another pattern to perform divergent functions.

To obtain some clues about the roles of *MiWRKY* genes in regulating the growth and development of the mango, the expression profile of *MiWRKYs* was analyzed in different tissues of the ‘Alphonso’ mango, including mature leaf, bark, seed, root, flower, peel, and flesh (Figure 6). A total of 27 *MiWRKYs* were highly expressed in most tissues (Group A), suggesting these WRKYs play essential roles in organ development. Since WRKY regulating plant development is mainly via transcriptional regulation of the target genes involved in physiological pathway [60], we assume that these highly expressed *MiWRKYs* may play a regulatory role in mango development, which needs to be further analyzed. Group B includes 24 genes specifically expressed in some particular tissues, which was also found in cassava [54], grape [5], cucumber [52], pineapple [4], and rice [15], suggesting WRKY proteins exhibit diverse functions in both monocotyledons and dicotyledons. In Group C, some genes, such as *MiWRKY60* and *MiWRKY71*, were hardly expressed in all the examined tissues, indicating they might play key roles in the development of other tissues. Genes, including *MiWRKY54*, *MiWRKY38*, and *MiWRKY73*, were only highly expressed in the root, suggesting these genes might contribute to the development of the root.

WRKY proteins are also involved in fruit anthocyanin accumulation. In the pear, PyWRKY26 and PybHLH3 could cotarget the *PyMYB114* promoter and activate the transcription of *PyMYB114* to regulate anthocyanin biosynthesis in the red-skinned pear cultivar, ‘Starkrimson’ [32]. In the apple, MdWRKY40 promotes wounding-induced anthocyanin biosynthesis by interacting with the MdMYB1 protein to increase the binding ability of MdMYB1 to anthocyanin biosynthetic genes [38]. Under UV-B conditions, MdWRKY72 promotes anthocyanin accumulation in the apple by activating *MdMYB1* expression directly by binding to a W-box motif in the *MdMYB1* promoter and indirectly by binding to a W-box element in the *MdHY5* promoter [37]. MdWRKY1 is involved in the early-stage light-induced anthocyanin accumulation in apple fruit by up-regulating the expression of a long noncoding RNA, *MdLNC499*, which in turn induces *MdERF109*; *MdERF109* subsequently induces the expression of anthocyanin biosynthetic and regulatory genes, including *MdCHS*, *MdUFGT*, and *MdbHLH3* [36]. In this study, *MiWRKY1*, *MiWRKY3*, *MiWRKY5*, *MiWRKY81*, and *MiWRKY84* were highly expressed in the red mango cultivar, ‘Guifei’, compared to the yellow or green cultivar, suggesting these WRKYs might be involved in the anthocyanin accumulation of the red-skinned mango. Meanwhile, *MiWRKY1* and *MiWRKY81* were significantly repressed by bagging treatment and induced by UV-B/visible light treatment, indicating these two WRKY genes might play important roles in regulating light-induced anthocyanin accumulation in the mango.

## 5. Conclusions

A total of 87 WRKY genes were identified from the mango genome and further classified into three main groups (Group I, II, and III) and five subgroups of Group II (a, b, c, d, and e), with high similarity in exon–intron structures and WRKY domain and motif compositions within the same group and subgroup. One tandem duplication (*MiWRKY76* and *MiWRKY82*) and 97 pairs of segmental duplicates were identified in the mango genome. Syntenic analysis showed that mango *MiWRKY* genes had 52 and 69 pairs orthologous with Arabidopsis and citrus, respectively. A large number of cis-acting elements associated with light-signaling, hormone response, environmental stress, and plant development were detected in the promoter region of *MiWRKYs*. The essential role of *MiWRKY* genes in regulating mango growth and development was implied by tissue-specific expression analysis. In addition, *MiWRKY1*, *MiWRKY3*, *MiWRKY5*, *MiWRKY81*, and *MiWRKY84* might regulate anthocyanin accumulation in red-skinned mango due to their high expression in the red mango cultivar, ‘Guifei’. The expression of *MiWRKY1* and *MiWRKY81* were induced by light, indicating their possible roles in light-induced anthocyanin biosynthesis in the mango. Our results provide a solid foundation to further investigate the function of WRKY in regulating anthocyanin biosynthesis in the mango.

**Supplementary Materials:** The following supporting information can be downloaded at: <https://www.mdpi.com/article/10.3390/agriculture12060821/s1>, File S1: Conserved domain sequences of 87 *MiWRKY* and 8 *AtWRKY* proteins used in this study; File S2: Sequences of the primers used in this study; File S3: List of the 87 *MiWRKY* genes identified in this study; File S4: Analysis and distribution of conserved motifs in mango WRKY proteins; File S5: Segmentally and tandemly duplicated *MiWRKY* gene pairs; File S6: One-to-one orthologous relationships between mango and other two plant species; File S7: Details of all the cis-acting elements in the promoter region of *MiWRKYs*; File S8: Public RNA-seq data of 87 *MiWRKY* genes that were used in this study; File S9: RNA-seq data of 6 *MiWRKY* genes that were used in this study.

**Author Contributions:** Conceptualization, B.S., H.W. and M.Q.; methodology, B.S., H.W., W.Z., B.Z., S.W. and K.Z.; data curation, B.S., H.W. and M.Q.; writing—original draft preparation, B.S., H.W., W.Z., B.Z., S.W., K.Z. and M.Q.; writing—review and editing, B.S., H.W. and M.Q.; funding acquisition, H.W. and M.Q. All authors have read and agreed to the published version of the manuscript.

**Funding:** This research was funded by the Major Science and Technology Plan of Hainan Province (grant number: ZDKJ2021014), National Natural Science Foundation of China (grant number: 32160678), Hainan Provincial Natural Science Foundation of China (grant number: 320QN192), the National Key Research and Development Plan of China (grant numbers: 2018YFD1000504; 2019YFD1000504), and the Scientific Research Foundation of Hainan University (grant number: KYQD(ZR)20053).

**Institutional Review Board Statement:** Not applicable.

**Informed Consent Statement:** Not applicable.

**Data Availability Statement:** The reported data can be found in Supplementary Materials.

**Conflicts of Interest:** The authors declare no conflict of interest.

## References

1. Rushton, P.J.; Somssich, I.E.; Ringler, P.; Shen, Q.J. WRKY transcription factors. *Trends Plant Sci.* **2010**, *15*, 247–258. [[CrossRef](#)]
2. Eulgem, T.; Rushton, P.J.; Robatzek, S.; Somssich, I.E. The WRKY superfamily of plant transcription factors. *Trends Plant Sci.* **2000**, *5*, 199–206. [[CrossRef](#)]
3. Wu, K.L.; Guo, Z.J.; Wang, H.H.; Li, J. The WRKY family of transcription factors in rice and Arabidopsis and their origins. *DNA Res.* **2005**, *12*, 9–26. [[CrossRef](#)] [[PubMed](#)]
4. Xie, T.; Chen, C.; Li, C.; Liu, J.; Liu, C.; He, Y. Genome-wide investigation of WRKY gene family in pineapple: Evolution and expression profiles during development and stress. *BMC Genomics* **2018**, *19*, 490. [[CrossRef](#)]
5. Wang, M.; Vannozzi, A.; Wang, G.; Liang, Y.H.; Torielli, G.B.; Zenoni, S.; Cavallini, E.; Pezzotti, M.; Cheng, Z.M. Genome and transcriptome analysis of the grapevine (*Vitis vinifera* L.) WRKY gene family. *Hort. Res.* **2014**, *1*, 16. [[CrossRef](#)]
6. Chi, Y.; Yang, Y.; Zhou, Y.; Zhou, J.; Fan, B.; Yu, J.Q.; Chen, Z. Protein–Protein interactions in the regulation of WRKY transcription factors. *Mol. Plant* **2013**, *6*, 287–300. [[CrossRef](#)]

7. Ishiguro, S.; Nakamura, K. Characterization of a cDNA encoding a novel DNA-binding protein, SPF1, that recognizes SP8 sequences in the 5' upstream regions of genes coding for sporamin and  $\beta$ -amylase from sweet potato. *Mol. Gen. Genet.* **1994**, *244*, 563–571. [[CrossRef](#)] [[PubMed](#)]
8. Ross, C.A.; Liu, Y.; Shen, Q.J. The WRKY gene family in rice (*Oryza sativa*). *J. Integr. Plant Biol.* **2007**, *49*, 827–842. [[CrossRef](#)]
9. Cai, C.; Niu, E.; Du, H.; Zhao, L.; Feng, Y.; Guo, W. Genome-wide analysis of the WRKY transcription factor gene family in *Gossypium raimondii* and the expression of orthologs in cultivated tetraploid cotton. *Crop J.* **2014**, *2*, 87–101. [[CrossRef](#)]
10. Huang, X.; Li, K.; Xu, X.; Yao, Z.; Jin, C.; Zhang, S. Genome-wide analysis of WRKY transcription factors in white pear (*Pyrus bretschneideri*) reveals evolution and patterns under drought stress. *BMC Genomics* **2015**, *16*, 1104. [[CrossRef](#)] [[PubMed](#)]
11. Meng, D.; Li, Y.; Bai, Y.; Li, M.; Cheng, L. Genome-wide identification and characterization of WRKY transcriptional factor family in apple and analysis of their responses to waterlogging and drought stress. *Plant Physiol. Biochem.* **2016**, *103*, 71–83. [[CrossRef](#)]
12. Zhang, C.Q.; Xu, Y.; Lu, Y.; Yu, H.X.; Gu, M.H.; Liu, Q.Q. The WRKY transcription factor OsWRKY78 regulates stem elongation and seed development in rice. *Planta* **2011**, *234*, 541–554. [[CrossRef](#)] [[PubMed](#)]
13. Yu, Y.; Hu, R.; Wang, H.; Cao, Y.; He, G.; Fu, C.; Zhou, G. MiWRKY12, a novel Miscanthus transcription factor, participates in pith secondary cell wall formation and promotes flowering. *Plant Sci.* **2013**, *212*, 1–9. [[CrossRef](#)] [[PubMed](#)]
14. Robatzek, S.; Somssich, I.E. A new member of the Arabidopsis WRKY transcription factor family, AtWRKY6, is associated with both senescence- and defence-related processes. *Plant J.* **2001**, *28*, 123–133. [[CrossRef](#)] [[PubMed](#)]
15. Ramamoorthy, R.; Jiang, S.Y.; Kumar, N.; Venkatesh, P.N.; Ramachandran, S. A comprehensive transcriptional profiling of the WRKY gene family in rice under various abiotic and phytohormone treatments. *Plant Cell Physiol.* **2008**, *49*, 865–879. [[CrossRef](#)]
16. Chen, L.; Song, Y.; Li, S.; Zhang, L.; Zou, C.; Yu, D. The role of WRKY transcription factors in plant abiotic stresses. *BBA Gene Regul. Mech.* **2012**, *1819*, 120–128. [[CrossRef](#)]
17. Banerjee, A.; Roychoudhury, A. WRKY Proteins: Signaling and regulation of expression during abiotic stress responses. *Sci. World J.* **2015**, *2015*, 807560. [[CrossRef](#)] [[PubMed](#)]
18. Petroni, K.; Tonelli, C. Recent advances on the regulation of anthocyanin synthesis in reproductive organs. *Plant Sci.* **2011**, *181*, 219–229. [[CrossRef](#)] [[PubMed](#)]
19. Holton, T.A.; Cornish, E.C. Genetics and biochemistry of anthocyanin biosynthesis. *Plant Cell* **1995**, *7*, 1071–1083. [[CrossRef](#)]
20. Allan, A.C.; Hellens, R.P.; Laing, W.A. MYB transcription factors that colour our fruit. *Trends Plant Sci.* **2008**, *13*, 99–102. [[CrossRef](#)]
21. Xu, W.; Dubos, C.; Lepiniec, L. Transcriptional control of flavonoid biosynthesis by MYB–bHLH–WDR complexes. *Trends Plant Sci.* **2015**, *20*, 176–185. [[CrossRef](#)]
22. Jaakola, L. New insights into the regulation of anthocyanin biosynthesis in fruits. *Trends Plant Sci.* **2013**, *18*, 477–483. [[CrossRef](#)]
23. An, J.P.; Qu, F.J.; Yao, J.F.; Wang, X.N.; You, C.X.; Wang, X.F.; Hao, Y.J. The bZIP transcription factor MdHY5 regulates anthocyanin accumulation and nitrate assimilation in apple. *Hort. Res.* **2017**, *4*, 17023. [[CrossRef](#)] [[PubMed](#)]
24. Zhou, H.; Wang, K.L.; Wang, H.; Gu, C.; Dare, A.P.; Espley, R.V.; He, H.; Allan, A.C.; Han, Y. Molecular genetics of blood-fleshed peach reveals activation of anthocyanin biosynthesis by NAC transcription factors. *Plant J.* **2015**, *82*, 105–121. [[CrossRef](#)]
25. Gou, J.Y.; Felippes, F.F.; Liu, C.J.; Weigel, D.; Wang, J.W. Negative regulation of anthocyanin biosynthesis in Arabidopsis by a miR156-targeted SPL transcription factor. *Plant Cell* **2011**, *23*, 1512–1522. [[CrossRef](#)] [[PubMed](#)]
26. Qian, M.; Ni, J.; Niu, Q.; Bai, S.; Bao, L.; Li, J.; Sun, Y.; Zhang, D.; Teng, Y. Response of miR156–SPL Module during the red peel coloration of bagging-treated Chinese sand pear (*Pyrus pyrifolia* Nakai). *Front. Physiol.* **2017**, *8*, 550. [[CrossRef](#)]
27. Ni, J.; Bai, S.; Zhao, Y.; Qian, M.; Tao, R.; Yin, L.; Gao, L.; Teng, Y. Ethylene response factors Pp4ERF24 and Pp12ERF96 regulate blue light-induced anthocyanin biosynthesis in 'Red Zaosu' pear fruits by interacting with MYB114. *Plant Mol. Biol.* **2019**, *99*, 67–78. [[CrossRef](#)]
28. Ni, J.; Premathilake, A.T.; Gao, Y.; Yu, W.; Tao, R.; Teng, Y.; Bai, S. Ethylene-activated PpERF105 induces the expression of the repressor-type R2R3-MYB gene *PpMYB140* to inhibit anthocyanin biosynthesis in red pear fruit. *Plant J.* **2021**, *105*, 167–181. [[CrossRef](#)]
29. Bai, S.; Tao, R.; Yin, L.; Ni, J.; Yang, Q.; Yan, X.; Yang, F.; Guo, X.; Li, H.; Teng, Y. Two B-box proteins, PpBBX18 and PpBBX21, antagonistically regulate anthocyanin biosynthesis via competitive association with *Pyrus pyrifolia* ELONGATED HYPOCOTYL 5 in the peel of pear fruit. *Plant J.* **2019**, *100*, 1028–1223. [[CrossRef](#)]
30. Bai, S.; Tao, R.; Tang, Y.; Yin, L.; Ma, Y.; Ni, J.; Yan, X.; Yang, Q.; Wu, Z.; Zeng, Y. BBX16, a B-box protein, positively regulates light-induced anthocyanin accumulation by activating MYB10 in red pear. *Plant Biotechnol. J.* **2019**, *17*, 1985–1997. [[CrossRef](#)] [[PubMed](#)]
31. Jaakola, L.; Poole, M.; Jones, M.O.; Kämäräinen-Karppinen, T.; Koskimäki, J.J.; Hohtola, A.; Häggman, H.; Fraser, P.D.; Manning, K.; King, G.J. A SQUAMOSA MADS box gene involved in the regulation of anthocyanin accumulation in bilberry fruits. *Plant Physiol.* **2010**, *153*, 1619–1629. [[CrossRef](#)]
32. Li, C.; Wu, J.; Hu, K.D.; Wei, S.W.; Sun, H.Y.; Hu, L.Y.; Han, Z.; Yao, G.F.; Zhang, H. PyWRKY26 and PybHLH3 cotargeted the *PpMYB114* promoter to regulate anthocyanin biosynthesis and transport in red-skinned pears. *Hort. Res.* **2020**, *7*, 37. [[CrossRef](#)]
33. Zhang, T.; Xu, H.; Yang, G.; Wang, N.; Zhang, J.; Wang, Y.; Jiang, S.; Fang, H.; Zhang, Z.; Chen, X. Molecular mechanism of MYB111 and WRKY40 involved in anthocyanin biosynthesis in red-fleshed apple callus. *Plant Cell Tiss. Org.* **2019**, *139*, 467–478. [[CrossRef](#)]
34. Zhang, H.; Zhang, Z.; Zhao, Y.; Guo, D.; Zhao, X.; Gao, W.; Zhang, J.; Song, B. *StWRKY13* promotes anthocyanin biosynthesis in potato (*Solanum tuberosum*) tubers. *Funct. Plant Biol.* **2022**, *49*, 102–114. [[CrossRef](#)]

35. Mao, Z.; Jiang, H.; Wang, S.; Wang, Y.; Yu, L.; Zou, Q.; Liu, W.; Jiang, S.; Wang, N.; Zhang, Z. The MdHY5-MdWRKY41-MdMYB transcription factor cascade regulates the anthocyanin and proanthocyanidin biosynthesis in red-fleshed apple. *Plant Sci.* **2021**, *306*, 110848. [[CrossRef](#)] [[PubMed](#)]
36. Ma, H.; Yang, T.; Li, Y.; Zhang, J.; Wu, T.; Song, T.; Yao, Y.; Tian, J. The long noncoding RNA MdLNC499 bridges MdWRKY1 and MdERF109 function to regulate early-stage light-induced anthocyanin accumulation in apple fruit. *Plant Cell* **2021**, *33*, 3309–3330. [[CrossRef](#)] [[PubMed](#)]
37. Hu, J.; Fang, H.; Wang, J.; Yue, X.; Su, M.; Mao, Z.; Zou, Q.; Jiang, H.; Guo, Z.; Yu, L.; et al. Ultraviolet B-induced MdWRKY72 expression promotes anthocyanin synthesis in apple. *Plant Sci.* **2020**, *292*, 110377. [[CrossRef](#)]
38. An, J.P.; Zhang, X.W.; You, C.X.; Bi, S.Q.; Wang, X.F.; Hao, Y.J. MdWRKY40 promotes wounding-induced anthocyanin biosynthesis in association with MdMYB1 and undergoes MdbT2-mediated degradation. *New Phytol.* **2019**, *224*, 380–395. [[CrossRef](#)]
39. Kour, R.; Singh, M.; Gill, P.P.S.; Jawandha, S.K. Ripening quality of Dusehri mango in relation to harvest time. *J. Food Sci. Technol.* **2018**, *55*, 2395–2400. [[CrossRef](#)]
40. Shi, B.; Wu, H.; Zheng, B.; Qian, M.; Gao, A.; Zhou, K. Analysis of light-independent anthocyanin accumulation in mango (*Mangifera indica* L.). *Horticulturae* **2021**, *7*, 423. [[CrossRef](#)]
41. Kanzaki, S.; Ichihi, A.; Tanaka, A.; Fujishige, S.; Koeda, S.; Shimizu, K. The R2R3-MYB transcription factor MiMYB1 regulates light dependent red coloration of ‘Irwin’ mango fruit skin. *Sci. Hortic.* **2020**, *272*, 109567. [[CrossRef](#)]
42. Kanzaki, S.; Kamikawa, S.; Ichihi, A.; Tanaka, Y.; Shimizu, K.; Koeda, S. Isolation of UDP: Flavonoid 3-O-glycosyltransferase (UGT)-like genes and expression analysis of genes associated with anthocyanin accumulation in mango ‘Irwin’ skin. *Hort. J.* **2019**, *88*, 435–443. [[CrossRef](#)]
43. Karanjalkar, G.R.; Ravishankar, K.V.; Shivashankara, K.S.; Dinesh, M.R.; Roy, T.K.; Sudhakar Rao, D.V. A study on the expression of genes involved in carotenoids and anthocyanins during ripening in fruit peel of green, yellow, and red colored mango cultivars. *Appl. Biochem. Biotechnol.* **2018**, *184*, 140–154. [[CrossRef](#)]
44. Karanjalkar, G.R.; Ravishankar, K.V.; Shivashankara, K.S.; Dinesh, M.R. Influence of bagging on color, anthocyanin and anthocyanin biosynthetic genes in peel of red colored mango Cv. ‘Lily’. *Erwerbs Obstbau.* **2018**, *60*, 281–287. [[CrossRef](#)]
45. Wang, P.; Luo, Y.; Huang, J.; Gao, S.; Zhu, G.; Dang, Z.; Gai, J.; Yang, M.; Zhu, M.; Zhang, H.; et al. The genome evolution and domestication of tropical fruit mango. *Genome Biol.* **2020**, *21*, 60. [[CrossRef](#)]
46. Chen, C.; Chen, H.; Zhang, Y.; Thomas, H.R.; Frank, M.H.; He, Y.; Xia, R. TBtools: An integrative toolkit developed for interactive analyses of big biological data. *Mol. Plant* **2020**, *13*, 1194–1202. [[CrossRef](#)] [[PubMed](#)]
47. Waterhouse, A.M.; Procter, J.B.; Martin, D.M.A.; Clamp, M.; Barton, G.J. Jalview version 2—A multiple sequence alignment editor and analysis workbench. *Bioinformatics* **2009**, *25*, 1189–1191. [[CrossRef](#)]
48. Kumar, S.; Stecher, G.; Li, M.; Niyaz, C.; Tamura, K. MEGA X: Molecular evolutionary genetics analysis across computing platforms. *Mol. Biol. Evol.* **2018**, *35*, 1547–1549. [[CrossRef](#)] [[PubMed](#)]
49. Wang, Y.; Tang, H.; DeBarry, J.D.; Tan, X.; Li, J.; Wang, X.; Lee, T.H.; Jin, H.; Marler, B.; Guo, H.; et al. MCSanX: A toolkit for detection and evolutionary analysis of gene synteny and collinearity. *Nucleic Acids Res.* **2012**, *40*, e49. [[CrossRef](#)] [[PubMed](#)]
50. Trapnell, C.; Roberts, A.; Goff, L.; Pertea, G.; Kim, D.; Kelley, D.R.; Pimentel, H.; Salzberg, S.L.; Rinn, J.L.; Pachter, L. Differential gene and transcript expression analysis of RNA-seq experiments with TopHat and Cufflinks. *Nat. Protoc.* **2012**, *7*, 562–578. [[CrossRef](#)]
51. Holub, E.B. The arms race is ancient history in Arabidopsis, the wildflower. *Nat. Rev. Genet.* **2001**, *2*, 516–527. [[CrossRef](#)] [[PubMed](#)]
52. Ling, J.; Jiang, W.; Zhang, Y.; Yu, H.; Mao, Z.; Gu, X.; Huang, S.; Xie, B. Genome-wide analysis of WRKY gene family in *Cucumis sativus*. *BMC Genomics* **2011**, *12*, 471. [[CrossRef](#)]
53. Wei, K.F.; Chen, J.; Chen, Y.F.; Wu, L.J.; Xie, D.X. Molecular phylogenetic and expression analysis of the complete WRKY transcription factor family in maize. *DNA Res.* **2012**, *19*, 153–164. [[CrossRef](#)]
54. Wei, Y.; Shi, H.; Xia, Z.; Tie, W.; Ding, Z.; Yan, Y.; Wang, W.; Hu, W.; Li, K. Genome-wide identification and expression analysis of the WRKY gene family in cassava. *Front. Plant Sci.* **2016**, *7*, 25. [[CrossRef](#)]
55. Xie, Z.; Zhang, Z.L.; Zou, X.; Huang, J.; Ruas, P.; Thompson, D.; Shen, Q.J. Annotations and functional analyses of the rice WRKY gene superfamily reveal positive and negative regulators of abscisic acid signaling in aleurone cells. *Plant Physiol.* **2005**, *137*, 176–189. [[CrossRef](#)]
56. van Verk, M.C.; Pappaioannou, D.; Neeleman, L.; Bol, J.F.; Linthorst, H.J.M. A novel WRKY transcription factor is required for induction of *PR-1a* gene expression by salicylic acid and bacterial elicitors. *Plant Physiol.* **2008**, *146*, 1983–1995. [[CrossRef](#)] [[PubMed](#)]
57. Zhou, Q.Y.; Tian, A.G.; Zou, H.F.; Xie, Z.M.; Lei, G.; Huang, J.; Wang, C.M.; Wang, H.W.; Zhang, J.S.; Chen, S.Y. Soybean WRKY-type transcription factor genes, *GmWRKY13*, *GmWRKY21*, and *GmWRKY54*, confer differential tolerance to abiotic stresses in transgenic Arabidopsis plants. *Plant Biotechnol. J.* **2008**, *6*, 486–503. [[CrossRef](#)]
58. Pandey, B.; Grover, A.; Sharma, P. Molecular dynamics simulations revealed structural differences among WRKY domain-DNA interaction in barley (*Hordeum vulgare*). *BMC Genomics* **2018**, *19*, 132. [[CrossRef](#)]

- 
59. Mackay, J.P.; Crossley, M. Zinc fingers are sticking together. *Trends Biochem. Sci.* **1998**, *23*, 1–4. [[CrossRef](#)]
  60. Sun, C.; Palmqvist, S.; Olsson, H.; Borén, M.; Ahlandsberg, S.; Jansson, C. A novel WRKY transcription factor, SUSIBA2, participates in sugar signaling in barley by binding to the sugar-responsive elements of the *iso1* promoter. *Plant Cell* **2003**, *15*, 2076–2092. [[CrossRef](#)]